

Dynamic triggering cases at the Salton Sea Geothermal Field in Southern California

Cameron Wang, Jianhua Gong, & Wenyuan Fan

IGPP, Scripps Institution of Oceanography, University of California San Diego

Abstract

The underlying physical mechanisms of dynamic triggering are not yet fully understood. We use the high-resolution Quake Template Matching catalog of Southern California to systematically evaluate dynamic triggering patterns at the Salton Sea Geothermal Field (SSGF). We apply a new data-driven statistical approach to the catalog to identify dynamic triggering cases, which can accommodate spatiotemporally evolving seismicity. We are particularly interested in the delayed triggering cases; categorizing the triggering responses of these cases may offer new insights into the physical mechanisms.

Regional and Global Data

Regional Seismicity Data at SSGF

We choose Southern California, and the SSGF specifically, because both are locations well-known for being highly seismically active. We take the region's seismicity data from the Quake Template Matching (QTM) catalog of earthquakes in Southern California covering the decade from 2008 to 2018. For this catalog, we take a magnitude of completeness of 0.5 from the point of maximum curvature of the SSGF's magnitude frequency distribution. We do not analyze events below this magnitude. Below is a sample SSGF seismicity plot around the time of the 2010 M_w 7.2 El Mayor Cucapah earthquake in Baja California.

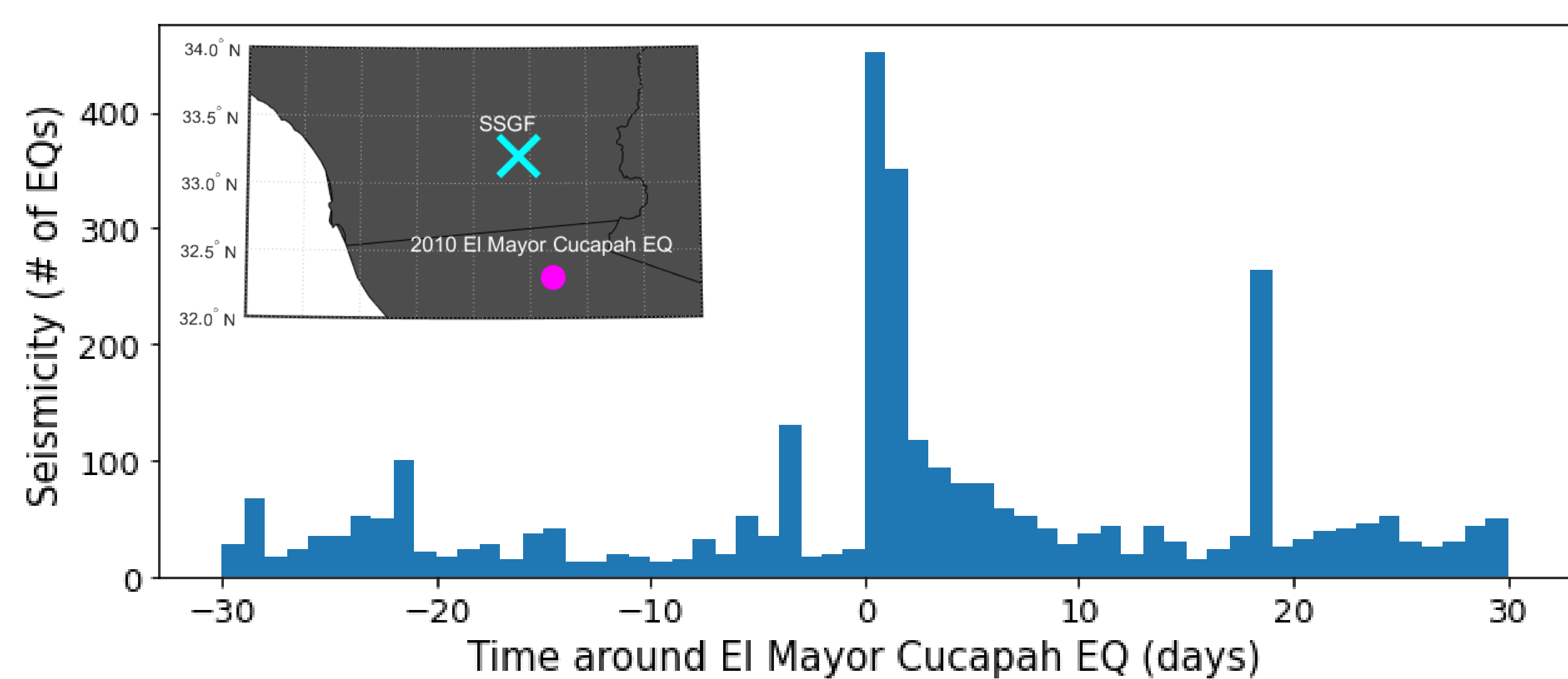


Figure 1: Sample seismicity of the SSGF (20 km radius), from 30 days before to 30 days after the 2010 M_w 7.2 El Mayor Cucapah earthquake.

Global Potential Triggers Data

We take all global events in the decade from 2008 to 2018 of $M_w \geq 6$ as potential triggering cases. Locations, origin times, and magnitudes of these events were obtained from the IRIS Data Management Center.

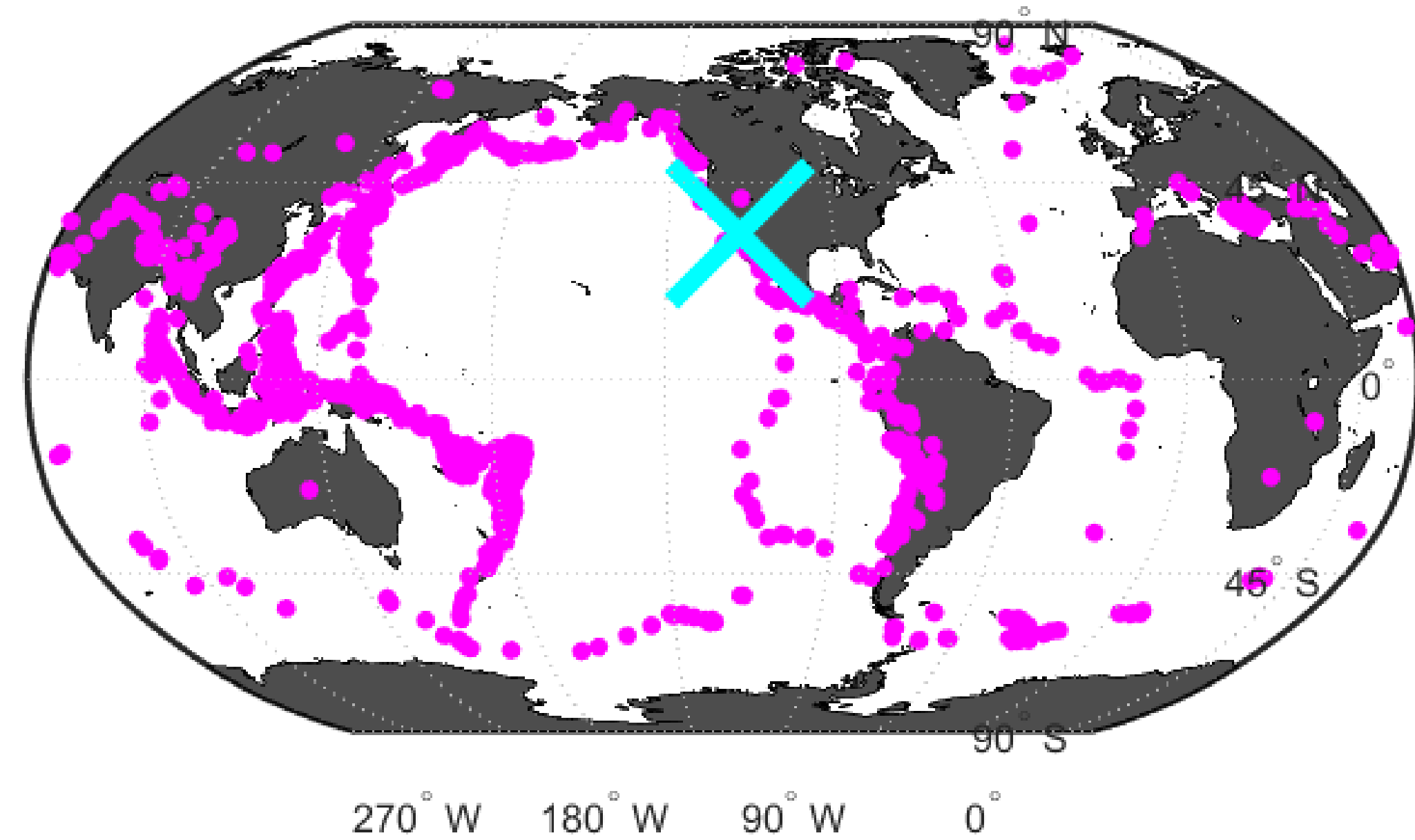


Figure 2: Global map of the SSGF (cyan X) and locations of all potential triggering cases (magenta circles).

Identifying Positive Cases

Seismicity rate changes: the β -statistic

We calculate a region's relative seismicity rate change using the β -statistic, defined as:

$$\beta = \frac{N_a - \Lambda}{\sqrt{\Lambda}}$$

Λ is an expected number of events, defined as:

$$\Lambda = N_b \frac{\delta t_a}{\delta t_b}$$

N_a is the number of events during a time period of interest δt_a , and N_b is the number of events during a background time period δt_b . Here, we take six different time periods of interest per case: timeframes of 2, 6, 12, 24, 72 hours, and 7 days after the potential trigger, with background time periods of 30 days before and after the potential trigger.

Thresholds of the β -statistic

A β -statistic ≥ 2 has been traditionally used to identify dynamic triggering. Here, we use a new statistical method proposed in Fan et. al. 2020 which adaptively determines triggering thresholds to account for changing seismicity. For each potential trigger, during each timeframe, four β -statistics are compared: β_0 , a β -statistic of interest; β_b , of equal length time period of interest before the potential trigger; $\beta_{95\%}$, the 95% confidence interval of a probability density function constructed from a distribution of 10,000 β -statistics of random time periods of interest within 30 days of the potential trigger; and $\beta_{5\%}^\Delta$, another confidence interval evaluated using a distribution of 10,000 β -statistics of random background time periods within 183 days of the potential trigger. An instance of dynamic triggering has occurred if there is a significant enough increase in seismicity, where β_0 is greater than β_b , $\beta_{95\%}$, and $\beta_{5\%}^\Delta$.

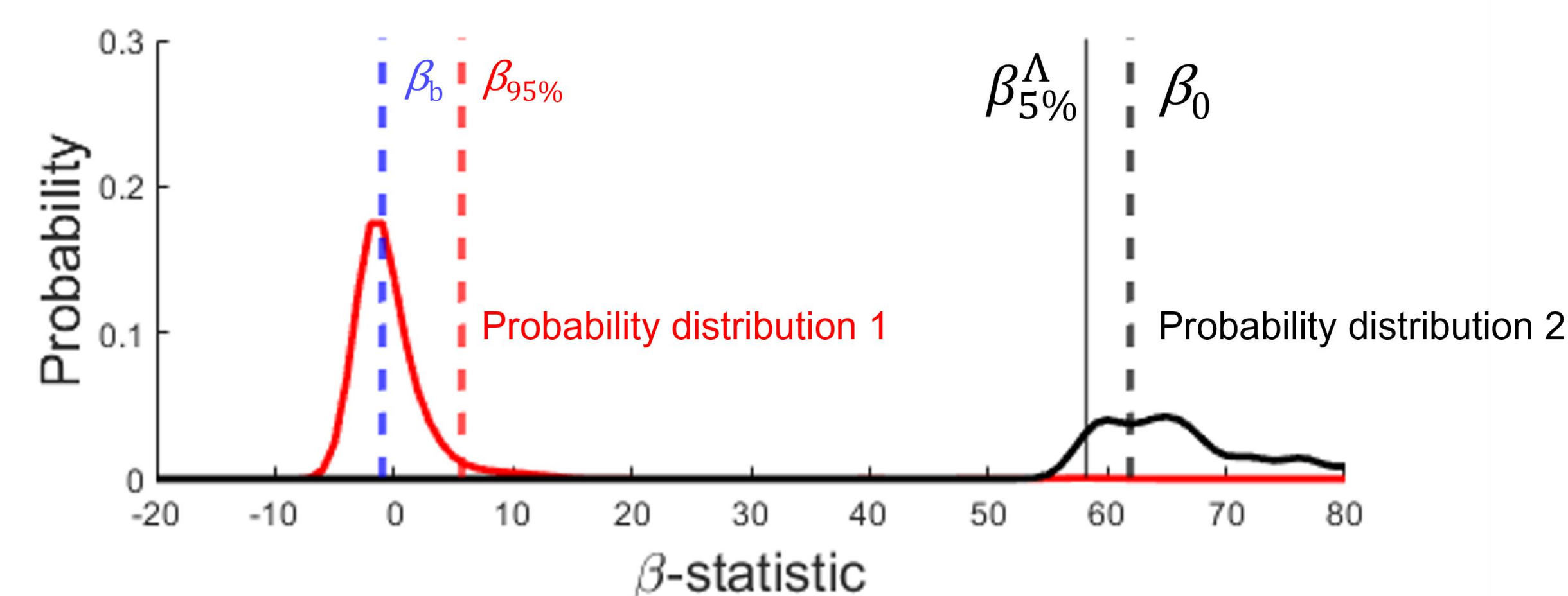


Figure 3: Sample 12-hour window of the El Mayor Cucapah earthquake. Because β_0 is further to the right than the other three β -statistics, dynamic triggering has occurred in this timeframe.

Results

We find a total of 1,419 potential triggers (150 of $M_w \geq 7.0$) valid for analysis. By the methods described, 153 of these potential cases (10 of $M_w \geq 7.0$) have dynamically triggered events at the SSGF. No earthquakes $M_w \geq 8.0$ dynamically triggered events at the SSGF.

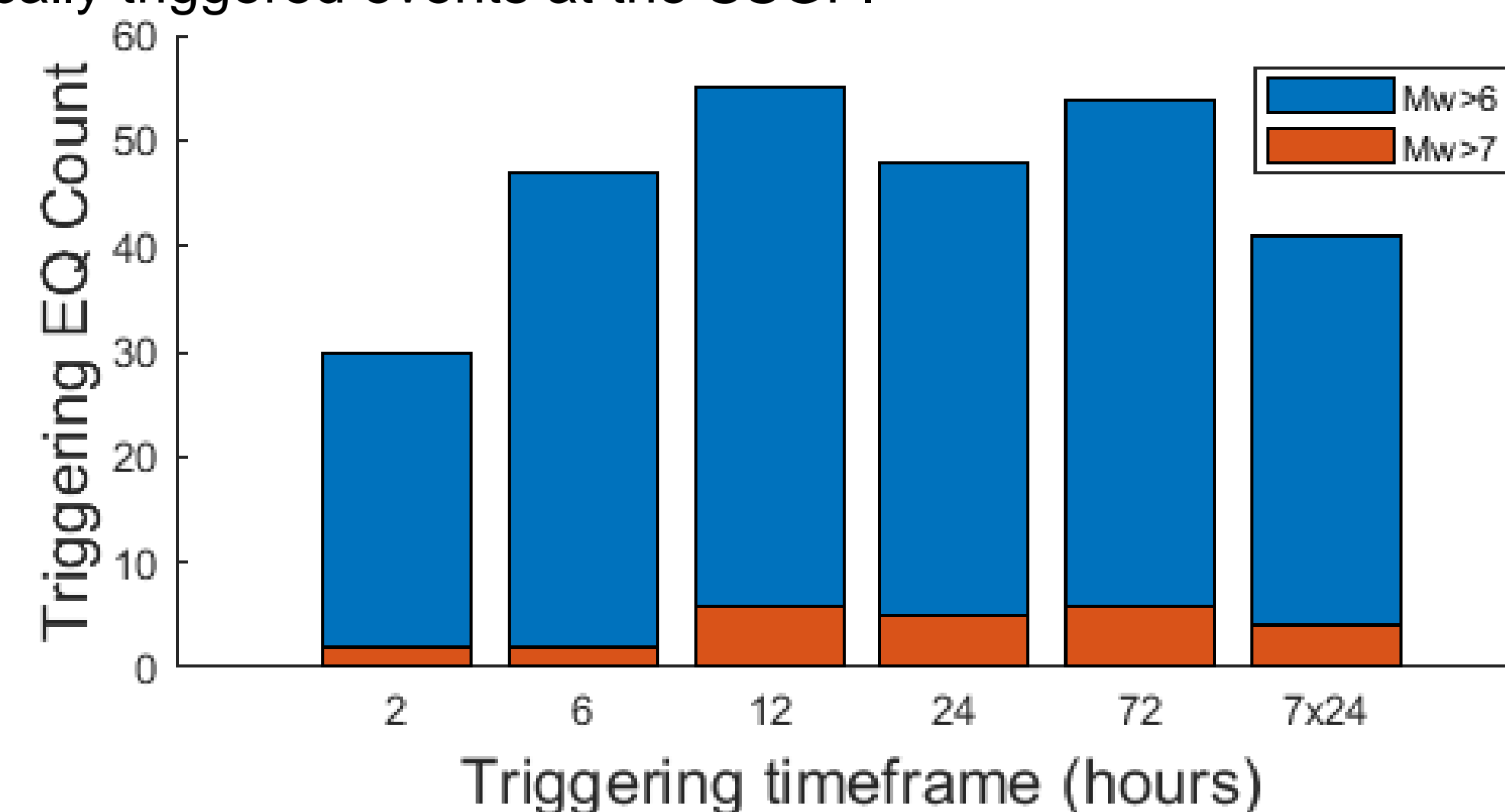


Figure 4: Positive cases by timeframe and magnitude totals, with magnitudes ≥ 7.0 in orange. Note that a case may show in multiple timeframes.

Triggering Responses

We identify both instantaneous triggering cases, where immediate triggering has occurred in the 2-hour timeframe (during the passing of seismic waves), and delayed triggering cases, where triggering has occurred in all other timeframes. Extended cases are defined where both instantaneous and delayed triggering has occurred.

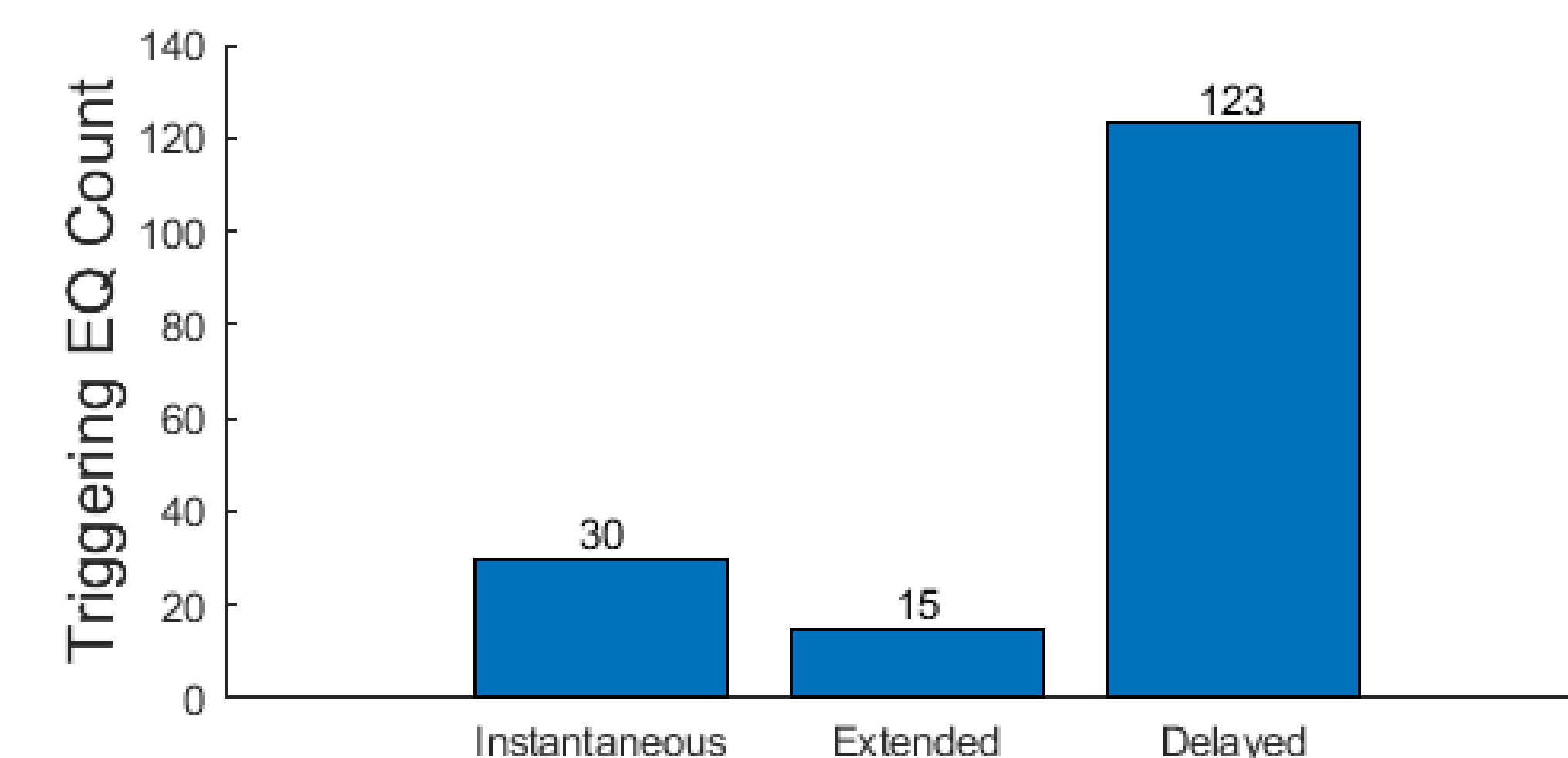


Figure 5: Positive cases by triggering mode.

123 of the 153 cases (80.4%) show delayed triggering, where the onset of increased seismicity occurs after the 2-hour mark. The remaining 30 cases (19.6%) show instantaneous triggering, half of which also have delayed responses and are therefore cases of extended triggering.

Azimuthal Distribution

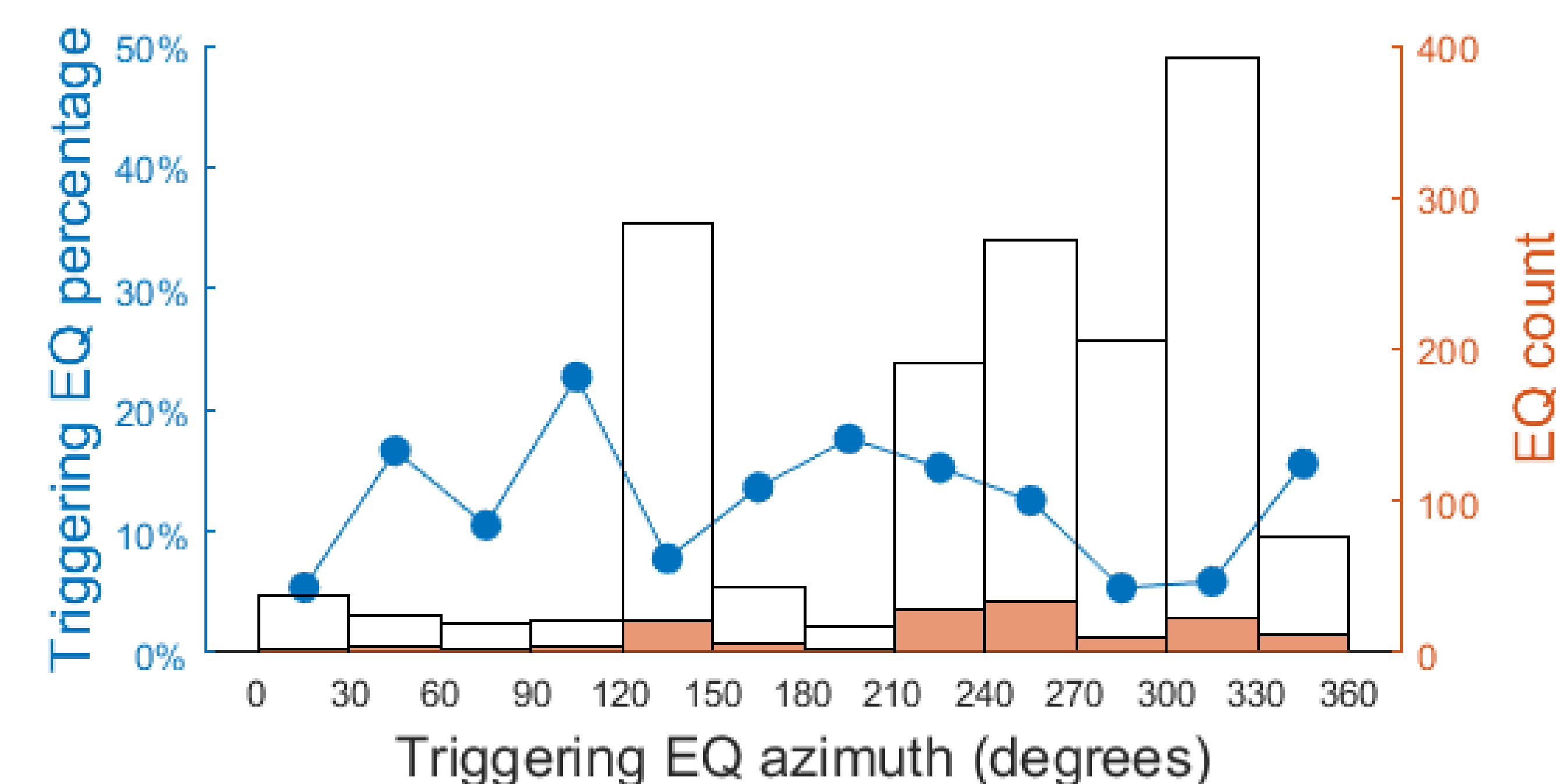


Figure 6: Azimuthal distribution of triggering cases – directions from the SSGF to the source location of potential trigger in 30° bins. Unshaded bars show all potential cases, shaded bars show positive cases, and blue points show ratios of positive cases to total cases.

We observe varying rates of triggering by back-azimuthal directions, where the directions of 30° - 60° , 90° - 120° , 180° - 210° , and 330° - 360° from the SSGF show higher percentages of triggering events to all events. Directions of 0° - 30° , 120° - 150° , and 270° - 300° show lower percentages.

Conclusion

- 153 of 1,419 potential triggers in 2008-2018 have dynamically triggered events at the SSGF.
- 30 events show instantaneous triggering, 123 show delayed triggering, and 15 show extended triggering.
- We observe varying rates of triggering by direction from the SSGF.
- Magnitude and distance of potential triggers may not be the only factors in dynamic triggering and other physical processes may be involved.
- We plan to continue analyzing these responses and apply this method to other geothermal fields to better understand this phenomenon.

References

- Fan, Wenyuan, et al. "Characteristics of Frequent Dynamic Triggering of Microearthquakes in Southern California." *Journal of Geophysical Research*, vol. 15, no. 1, 2020.
- Ross, Zachary E., et al. "Searching for hidden earthquakes in Southern California." *Science*, vol. 364, no. 6442, 2019, pp. 767-771.
- Kiib, Deborah, et al. "Triggering of earthquake aftershocks by dynamic stresses." *Nature*, vol. 408, no. 6812, 2000, pp. 570-574.
- Gomberg, J., et al. "Earthquake triggering by seismic waves following the Landers and Hector Mine earthquakes." *Nature*, vol. 411, no. 6836, 2001, pp. 462-466.
- Meng, Xiaofeng, & Zhigang Peng. "Seismicity rate changes in the Salton Sea Geothermal Field and the San Jacinto Fault Zone after the 2010 M_w 7.2 El Mayor-Cucapah earthquake." *Geophysical Journal International*, vol. 197, no. 3, 2014, pp. 1750-1762.